Babeș-Bolyai University Cluj-Napoca

Institute for Doctoral Studies

Doctoral School of Environmental Science

Geochemical characteristics of thermal and mineral waters in the Apuseni Mountains

Doctoral Thesis Summary

PhD Coordinator:

Prof. univ. dr. Călin Baciu

PhD Candidate:

Nicula Marius-Alin

Cluj-Napoca

2021

Contents

1.Introduction to the studied topic

1.1 Objectives of the study

The research carried out within the doctoral thesis started from the following objectives:

1. Determining the thermal water distribution in the study area.

2. Quantitative characterization, quantification of geothermal flows and calculation of their energy input.

3. Geochemical characterization of geothermal systems.

4. Explaining the genesis of these waters and creating the conceptual model (s) for the identified geothermal systems.

The doctoral thesis deals in a broad way with these objectives to obtain relevant conclusions, valid from a scientific point of view. In the chapter reserved for conclusions, each objective is treated punctually based on the data obtained and presented in the previous chapters.

1.2 Thesis structure

The thesis is structured in 7 main chapters. Chapter 1 provides a general description of the topics studied with emphasis on the legislative elements and the history of thermal exploitations in the Apuseni Mountains. Following these introductory elements, the objectives pursued in the doctoral thesis are stated.

Chapter 3 describes the study area, for the beginning a general geographical description of the area is made and subsequent a more detailed description of the relief units is made. In addition to the aspects of physical geography, the climatic status of the study area is also presented, the data regarding temperature and precipitation being important for the studied field. The geological and tectonic description of the study area is discussed in detail in this chapter. From the point of view of tectonics, the theories regarding the formation and dynamics of the Apuseni Mountains space are presented. The geological characterization is presented for each test area.

Chapter 3 presents information about geothermal waters provided by the bibliography. At the end of this chapter, we discuss the practical and economic applicability of geothermal waters.

Chapter 4 presents the research methodology. The first issues addressed in this chapter are related to field campaigns and the methodology of sampling and storage of water and gas samples. Subsequently, the analysis protocols for each type of measurement performed and the characteristics of the devices are described.

Chapter 5 presents the results obtained and at the same time the data obtained are interpreted to facilitate the understanding of the researched aspects. With the data obtained for the water samples (anions and cations) Piper, Stiff, Giggenbach diagrams were obtained, and the isotopic data are presented in different graphs. Diagrams are also used for data obtained from the measurement of gas samples to facilitate the interpretation of the results.

Chapter 6 presents the conclusions of the thesis and at the same time answers each objective stated in the first chapter. In the last chapter the bibliography is presented.

2. Characterization of the study area

The Apuseni Mountains are in the western part of Romania and represent a compact relief unit with considerable dimensions. This unit covers an area of approximately 5200 km2. In the southern part they are delimited by the Mureș River (Mureș Valley). South of this natural border are the Poiana Ruscă Mountains which are part of the Southern Carpathians. In the eastern part it borders the Transylvanian Depression, the border being more diverse and consisting of several specific subunits. In the western part, the boundary is not obvious, due to the special morphology of the western extremity of the Apuseni Mountains. In this western part there are three golf depressions (Vad-Borod, Beiuș and Zarandului) that fragment the mountain unit. A similar situation is found on the northern side of the Apuseni. In this case, the Șimleu Depression does not penetrate the mountain so much and allows a more correct delimitation. The Someș Valley and the contact with the Crasna and Sălaj hills can be considered as a limit (Ianovici et al., 1976).

Tectonics and formation of the Apuseni Mountains

One of the theories of the formation of the Apuseni Mountains is presented in the book Geotectonics of Romania, this theory describes subduction phenomena in the southern area of these mountains. These subduction phenomena intervened in the evolution of the Metaliferi Mountains and this fact also explains the island arcs in this area, generated by convergent subduction. The nappes from the Metaliferi Mountains are made up of magmatic rocks (ophiolithic complexes) and sedimentary rocks (carbonate type, flysch) being considered obduction generated nappes (Săndulescu, 1984).

Another model of the evolution of the Apuseni Mountains is described by Mutihac (1990). The genesis of these mountains is attributed to a rift that appeared on the Transylvanian-Pannonian microplate. The formation of these mountains divided the areas known today as the Pannonian Basin and the Transylvanian Basin. The geology of the Apuseni Mountains shows similarities with other branches of the Carpathians, this aspect may also suggest similarities in terms of genesis (Mutihac, 1990).

One of the most current theories on the genesis of the Apuseni Mountains is presented by Stefan M. Schmid in a complex paper on the tectonics of Eastern European space (Schmid et al., 2020). Currently, three major units are recognized inside the Carpathian arc: the ALCAPA block, the Tisia unit and the Dacia unit. Between the ALCAPA Block and the Tisia unit is the Maramureș - Szolnok corridor. The defining elements for the Apuseni Mountains are the Tisia and Dacia units. These two continental blocks advanced from the southwest to the interior of the Carpathian arc and through this advance pushed the oceanic plate previously present to the subduction zone in the Eastern Carpathians. This oceanic plate has subduced and melted, respectively, giving way to the tectonic units present at this moment. The Northern Apuseni identify with the unit of Tisia, present nappes of different ages, the most representative are the nappes of Codru and those of Biharia. Their genesis took place mainly between the Mesozoic and Neozoic.

The rocks that predominate in this mountain group are limestone, crystalline shales and granites. Souther Apuseni are largely characterized by the Dacia unit, being at the contact between the two major units in this area (Tisia and Dacia). Biharia nappes, Supragetic and Getic nappes are identified on their contents. In the Metaliferi Mountains, over the Biharia

nappes there are ophiolitic rocks. These rocks come from the oceanic crust between the Tisia and Dacia units. Due to the proximity between the two units, this crust was obtained over the nappes of Biharia, so that the ophiolitic complex cover the unit of Biharia. In the Southern Apuseni are also found: prehercine (M. Trascău) and hercynic crystalline shle (Rapolt Crystalline Island), prelaramic sediments, laramic magmatites, Neogene volcanites and Quaternary basaltic volcanites (Mutihac, 1990). The formation of this group took place between Jurassic and Cretaceous. Following the genetic stages described, there was a rotational movement of the major units clockwise. This rotation generated the formation of gulf depressions (Vad-Borod, Beiuș and Zarand) and favored the emergence of Neogene volcanism in the southern Apuseni. Due to the de-stressing caused by the rotation of tectonic units, the pressure decreased in some areas and allowed the rock melting temperature to decrease, which favoured the advance of the magma to the surface. This phenomenon seems to have been responsible for the stage of Neogene volcanism in the southern Apuseni (Seghedi et al., 2005). After these previously described steps, several layers of sediments were deposited in the Neogene, especially in the depression areas (Schmid et al., 2020).

3. Relevant aspects about geothermal waters

The Apuseni Mountains area was the concern of several researchers who undertook field campaigns and wrote scientific papers on this area. One of the first relevant works on this topic was published in Vienna in 1863 by Schmidl (Schmidl, 1863). This work creates a geological and geographical radiography of the Metaliferi Mountains, Bihor and Codru Moma. With the modernization and industrialization, the concern for this area increased, and after 1950 several studies were carried out on hydrological, hydrogeological, geological and geographical topics.

Heat fluxes in the study area are not recognized as having significant thermal potential. In the area of the Apuseni Mountains the temperature estimated at a depth of 20 km is 500 ° C (Demetrescu & Andreescu, 1994). The same study states that the units in the west have temperatures higher than 600 - 700 ° C and in the east for the same depth the temperatures are lower (300 - 400 ° C). For the Eastern Carpathians, the estimated temperatures are

higher than in the Apuseni Mountains and can reach 800 ° C in some areas. These thermal variations between the major structural units are confirmed by Tiliță et al. (2018) in a paper that addresses the heat flow related to the Transylvanian Basin.

In the literature were identified several references about geothermal manifestations in the Apuseni Mountains. These works are not mainly dedicated to the Apuseni Mountains, the study area is extended to larger areas. Butac & Opran (1985) provides some data on geothermal waters from Geoagiu, Vața and Moneasa, mentioning the flows and temperatures of the sources. Gheorghe & Crăciun (1993) present the main geothermal resources on the Romanian territory. The Apuseni Mountains are not considered a main area with geothermal deposits.

The regional geothermal context is presented in the synthesis paper "Mineral and Thermal Waters of Southeastern Europe" (Papic et al., 2016). A chapter of this paper presents considerations about geothermal waters in Romania. Of interest for the present study is the description of the geothermal deposit from Beiuș, characterized by waters with temperatures above 80°C and low mineralization.

One of the most complex and relevant works for hydrogeology in this area and implicitly for the present study is "Hydrogeology of the karst from the Apuseni Mountains" published by Orășeanu (2016).

In this book is described five predominant hydrogeological entities identified in the Apuseni Mountains. A first entity is identified with marly and clay deposits and flysch series. These types of deposits are characterized by variable permeabilities, and in some cases can accommodate small aquifers. A second category is represented by marls, clay shales, pebbles and Pleistocene or Holocene sands. Enlarge sedimentary deposits are characterized by high permeability and can create small aquifers. Another entity with a significant presence in this study area consists of Paleozoic granites and rhyolites, Mesozoic ophiolites, magmatites and vulcanites (laramic, Neogene, metamorphic). These areas may contain cracks that facilitate water circulation. The molasses deposits (clay shales, sandstones, conglomerates) represent the fourth hydrogeological entity reported in the Apuseni Mountains. Water flows through the cracks of these deposits, and in the absence of cracks or if the thickness of the deposits is larger, they can be waterproof barriers. The most

representative hydrogeological entity for the study area is represented by the Mesozoic and Paleozoic carbonate series. Areas with such deposits have an infiltration and intense groundwater circulation and can accommodate significant aquifers from a quantitative point of view. Waters move easily along cracks and dissolution voids (Orășeanu, 2016).

4. Use of geothermal water

At the national level, a significant percentage of the geothermal resources used are exploited for recreational and curative purposes (Antics & Roșca, 2003). If analyse the thermal waters from the point of view of hydro thermotherapy, we find that the reference temperature from which these waters have a pronounced effect is over 35◦C. This temperature is chosen for physiological reasons, considering that the “indifference” temperature is 34-35◦C (Rădulescu & Teodoreanu, 2014). Also, from a balneological point of view in the work "Manual of balneology", waters with a temperature higher than 20◦C are considered thermal and with therapeutic potential (Sturza, 1950).

Numerous uses and curative properties of these thermo-mineral waters are described in specialized works that have the theme of balneology and hydrotherapy. Both the physical and chemical properties are considered important. We will not go into details related to the therapeutic procedures themselves, but we consider it relevant for this study to list the main physiological actions that thermal baths have on the human body. Therapy with such waters is recommended for problems related to musculoskeletal, cardiovascular, respiratory, vegetative nervous system but also for stimulating and regulating renal function. For all these uses it is very important to know the source of the water and its qualitative content (Rădulescu & Teodoreanu, 2014; Sturza, 1950).

The thermal areas with curative properties that enter the area of this study and are mentioned and described from a balneological point of view in the Balneology Manual, are: Baile Felix, Moneasa, Vața Băi, Geoagiu and Călan (Sturza, 1950).

At present, in the study area in direct connection with the geothermal waters, the following resorts are known (from south to north): Călan, Geoagiu Băi, Vața Băi, Moneasa and Băile Felix.

Technical and economic applicability

Geothermal energy is renewable energy that has a low impact on the environment in the case of rational exploitation. The political and legislative trends promoted worldwide encourage compliance with the principle of sustainable development, and geothermal sources serve this goal. In addition to these ethical and legislative issues, the use of such a source can generate economic benefits.

Quantified data worldwide show that the interest in geothermal energy increase and at the same time the use of this resource has increased (IGA, 2020). The world's largest users of geothermal energy are: China, USA, Sweden, Turkey, Germany, and Iceland (Lund & Boyd, 2016).

From the point of view of domains of use there are many possibilities. In terms of the number of users, geothermal energy is used for heat pumps. After 2005, this type of use increased significantly due to technical progress in the field of heat pumps.

In order of the geothermal capacity used, the next sector is leisure and balneology. This sector has an ancient tradition and experiences a spectacular growth between 1995 and 2000 and then had a slightly upward trend. Agricultural use, represented by greenhouses and fish farming, has a lower share of the geothermal energy used. This sector had an upward trend during the period 1995 - 2015. The use of geothermal resources in industry did not progress significantly (Lund & Boyd, 2016; IGA, 2020).

One of the most visible and publicized uses is for tourist purposes (spa / curative). Many areas that have these resources have developed a specific tourism infrastructure and generate income from the exploitation of this resource. Thus, resorts are spread all over the planet. At European level, the Pannonian Basin area is famous for its balnear locations, as well as the resorts in Central Europe, along the Eger Rift. Countries such as Iceland, Hungary and Italy have a tradition of using this resource. At national level, eloquent examples in this sense can be found at: Herculane, Călimănești-Căciulata, Băile Felix, Băile Tușnad.

Another field suitable for the use of geothermal energy is agriculture. Geothermal fluxes can be used to heat greenhouses (Sordelli and Karkoulias, 1995; Berdondini et al., 1995). Geothermal flows with lower temperatures but consistent flows are suitable for this type of

use. Good results were obtained for vegetable greenhouses, and the optimal development of cultivated plants was achieved (Boyd & Lund, 2000). Geothermal waters are successfully used in maintaining a favourable environment to the development of different types of algae (Plugaru et al., 2018).

Fish farms can be a viable way to use geothermal resources. It is a practice that brings economic benefits in areas with a lower enthalpy. It is suitable for various species of fish that are viable for capitalization (Boyd & Lund, 2000). In such farms a high growth rate is obtained due to the extension of the period of activity and feeding of fish. In the national (temperate) climatic context, the stagnant period of the winter season can be eliminated. These fish farms can diversify cultivated species and acclimatize non-native species.

In the industrial field, geothermal fluxes can be used to generate heat. A common use is in the food industry, where these flows are used to dry some foods (Arason, 2003, Sordelli & Karkoulias, 1995).

One of the most common uses for geothermal energy is the heating of homes and public spaces. Technological progress has developed equipment that uses this energy. The technical, economic requirements of these heating systems have become sustainable for home users. Good energy efficiency and the possibility of amortizing the investment significantly increased the number of users.

The use of geothermal fluxes for electricity production is another use of this resource. Through this conversion process, geothermal energy can be stored and transported much more easily, without significant losses. This use is suitable for areas with a high enthalpy (approximately 120 °C). In the case of the area studied by us, this form of use is not viable, because the water temperature is below 100 °C and has a low enthalpy (Colesca & Ciocoiu, 2013).

5. Research methodology

Sampling methodology

Field campaigns

To achieve this research, 5 field campaigns were performed. The main purpose of these campaigns was the field investigation of water sources and collection of water and gas samples for the present study. Geological and geographical observations were made in the field, to get to know the study area as well as possible. Points with geothermal waters described in the literature have been identified.

Based on the data extracted from the specialized works, the indicative route of the field campaigns was established.

The study area was divided into two subzones strictly in terms of field campaigns. The first subzone is identified with the southern area of the Apuseni Mountains, and field campaigns were performed near the Mureș Valley (Călan, Geoagiu and Rapoltu Mare). In this subzone, 3 field campaigns were performed, the first of them in October 2018, the second in November 2019, and the last in December 2019. The second subzone is identified with the north-western part of the Apuseni Mountains and the gulf depressions (Vad-Borod, Beiuș and Zarandului) of these mountains. The field campaigns were performed in the proximity of the localities: Vața de Jos, Moneasa, Vașcău, Ștei, Beiuș, Băile Felix and Aleșd. Two field campaigns were performed in this area, in February 2019 and November 2019.

In the field campaigns described above, 42 points were identified and tested.

In the first subzone, 18 points relevant for the present study were identified and tested and in the second subzone 24 points. Most of the points presented in figure 1 is represented by drilling (28 drillings representing 66.6% of the total points). The second significant percentage is represented by springs (12 springs representing 28.5% of the total points). In addition to drilling and springs, geothermal water samples were taken from a lake (MA 9) and a well (MA 4). Figure 1 shows all these points and highlights the subzones.

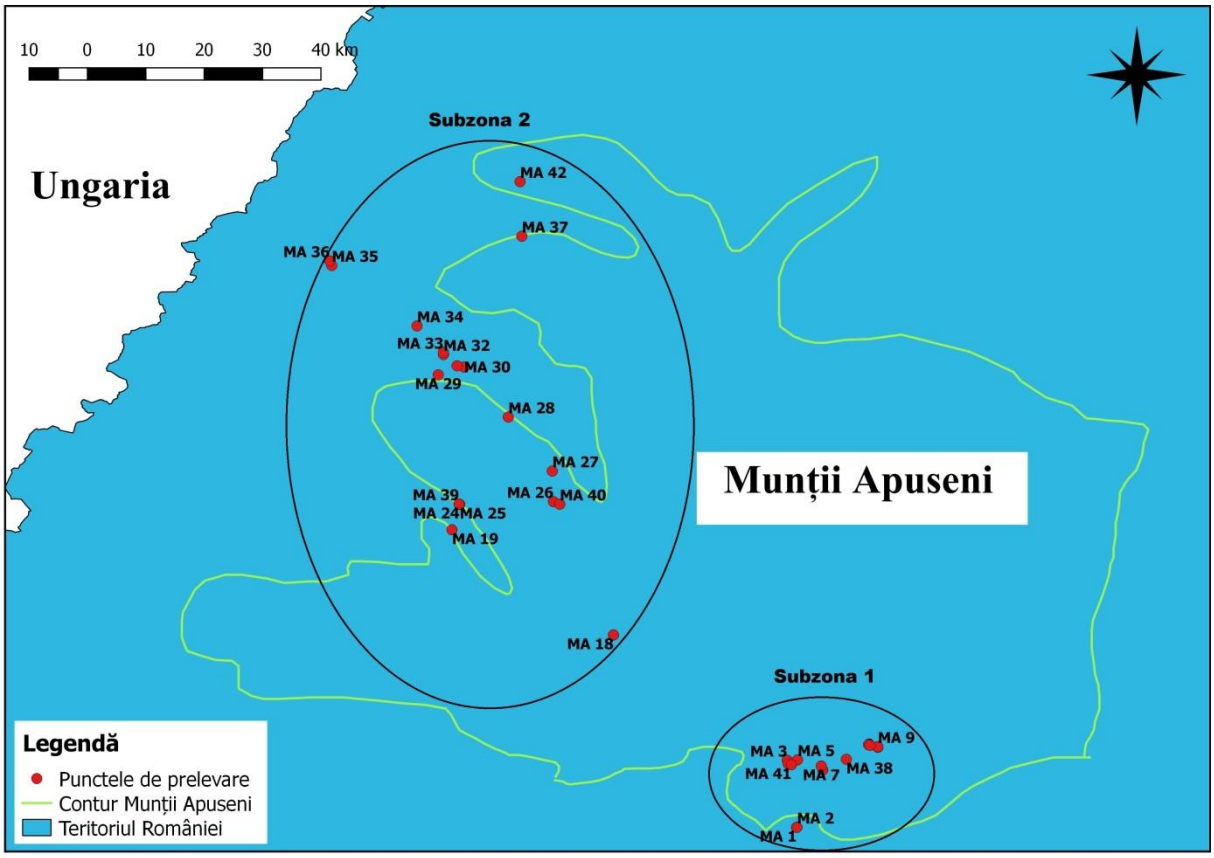

Figure 1. Positioning of sampling points

Water sampling

Samples were collected from the points described above. The samples were collected in polyethylene containers and glass bottles with a septum threaded stopper.

Samples were collected from the glass vials and subjected to isotopic analysis. Samples for the determination of heavy metals were collected in polyethylene containers and acidified with HCl to a pH of 2. Containers like those used in the sampling of heavy metals were also used in the samples for the determination of major ions. Water samples for TDIC (total dissolved inorganic carbon) analysis were taken from polyethylene flasks and NaOH + $BaCl_2$ was added.

During each sampling campaign, the following information was noted for the samples collected: the name of the person who collected, the locality, the name of the water source, the date, the place of collection, the use of water and the type of the analysis proposed. After this action, the samples were stored in an isolation box. Subsequently, the samples were transported to the Faculty of Environmental Science and Engineering, and stored in the

refrigerator at a temperature of approximately 4°C. After a part of the sample were measured in the laboratory or sent to partners for measurements.

Sampling for gas analysis

Samples were collected for the determination of gases dissolved in water according to the methodology described by Italiano et. al., (2014). Samples were collected thoroughly to avoid contamination with atmospheric air. After the field campaign samples were packaged and then sent for analysis to the National Institute of Geophysics and Volcanology (INGV) Palermo.

For the isotopic determination of the dissolved gases He (^{3}He / ^{4}He) and Ne (^{20}Ne / ^{22}Ne), the samples were collected in copper pipes. The sampling was collected with the help of a rubber hose and the whole device included two metal clamps to achieve the tightness of the system. These samples were sent for analysis to the Isotope Climatology and Environmental Research Centre (ICER), Debrecen, Hungary.

Free gas samples were performed depending on the presence of gases and the availability of point testing. At the points where the samples could be performed, a funnel was used to easily capture the free gas emissions.

In-situ measurements and activities

During this research, several in-situ activities were performed. After arriving in the established areas, an analysis of the area was performed from a geographical and geological point of view (geographical coordinates and relevant information about the location). To identify some sources the field team talked to the locals. We walked through the areas near the points to identify information relevant to the present study.

Where there was a possibility, the source flow was measured. With a WTW 350i multiparameter we measured some parameters (pH, temperature, dissolved oxygen, electro-conductivity, total dissolved solids, redox potential, and salinity) at the source.

The determination of bicarbonates was performed in-situ by the titrimetric method, using a microdozimeter. The substances used for this operation were hydrochloric acid and methyl orange.

Subsequently, water and gas samples were taken according to the methodology described above.

Methodology for measuring the collected samples

Water

Determination of main ions

The water samples collected to determine the main ions were filtered, with 0.45 µm filters. A dilution with ultrapure water was then performed to bring the samples to a conductivity of about 100 µS / cm.

An ion chromatography system (Dionex 1500 IC, USA) was used for samples analysis. The ion chromatograph system was equipped with 4 × 250 mm IonPac AS23 and CS12A columns, 4 × 50 mm IonPac A23G and CG12A pre-columns and self-regenerating suppressor (ASRS ultra II / CSRS ultra II, 4 mm). The concentration of the following elements was achieved with this apparatus: (Br^-, NO_2^-, F^-, Cl^-, NO_3^-, PO_4^{3-}, SO_4^{2-}, Li^+, Na^+, K^+, NH^{4+}, Mg^{2+}, Ca^{2+}). The eluents used for the analysis process were 4.5 mM Na2CO3 / 0.8 mM NaHCO3 (for anions) and 20 mM metasulfonic acid (99.0%) (for cations), with a flow rate of 1 mL / min. The calibration curves were performed using the calibration curves represented for six standard solutions prepared by serial dilutions of the stock solutions: Dionex™ Combined Seven Anion Standard II / 057590 and Dionex™ Combined Six Cation Standard-II / 046070. The method had a linearity of R2> 0.999. The detection limits have the following values: 10.3 µg/L (Li^+), 12.2 µg/L (Na^+), 11.9 µg/L (NH_4^+), 12.7 µg/L (K^+), 11.8 µg/L (Mg^{2+}), 17.1 µg/L (Ca^{2+}), 10.1 µg/L (F^-), 21.2 µg/L (Cl^-), 11.4 µg/L (NO_2^-), 12.4 µg/L (Br^-), 12.0 µg/L (NO_3^-), 15.8 µg/L (PO_4^{3-}), 12.7 µg/L (SO_4^{2-}).

Determination of heavy metals

Before analysis, the samples were filtered (0.45 µm) and acidified with 65% HNO3 nitric acid (Merk) to obtain a pH around 2. The analysis of the samples was done using a ZEEnit 700

Analytik Jena system equipped with air and acetylene burner, graphite furnace and special cathode lamp for each metal. The metals analysed for this study are: Pb, Fe, Zn, Ni, Cd, Cu, Cr.

The calibration curves were obtained using six standard solutions prepared by serial dilutions from a standard multi-element ICP solution (1000 mg / L, standard IV / 111355, Merck). The method has a linearity expressed by the mathematical relation (R2> 0.999), this relation expresses a good accuracy of the measurements performed by the device. For the flame determination method, the limits of detection are: 12 µg/L (Fe), 35 µg/L (Cr), 12 µg/L (Cd), 38 µg/L (Ni), 13 µg/L (Zn), 83 µg/L (Pb) and 36 µg/L (Cu). For samples that have a lower concentration of metals, it is possible to opt for the atomization technique in a graphite furnace. This method is suitable for such samples because it has lower detection limits: (0.08 µg /L for Cd and 0.66 for Ni µg /L).

Determination of isotopes

The determination of the isotopes from the water samples was performed with a Picarro L2130-I device from the Stable Isotopes Laboratory of Babeș-Bolyai University. This device uses CRDS technology, which allows the simultaneous measurement of $\delta^{18}O$ and $\delta^{2}H$. The accuracy of the measurements is <0.025 ‰ for $\delta^{18}O$ and for $\delta^{2}H$ it is <0.1 ‰ (https://www.picarro.com; Dumitru et. al., 2016).

The standard methodology recommended by the manufacturer was used, which requires 2 ml of the re-filtered sample on a 0.22 µm filter. The measurements were performed according to IAEA Vienna standards. The data obtained are presented according to the formula: δ (‰) = (Rsample / Rstandard -1) * 1000.

Determination of TDIC

Samples were collected for the determination of TDIC ($\delta^{13}C$) in polyethylene vials (50 ml). After the actual sampling, NaOH and $BaCl_2$ were added to precipitate the carbonates. The samples brought from the field were placed in the oven at the Faculty of Environmental Science and Engineering and kept until the complete evaporation of the liquid fraction.

Subsequently, the solid fraction remaining on the walls of the vessel was detached and the resulting dust was stored in sealed envelopes.

The analysis (TDIC) of this dust was performed in the geochemistry laboratory of INGV-Naples, Italy. The device used to perform these measurements was a Delta PlusXP (MS) continuous flow mass spectrometer coupled to a GasbenchII (GBII) device. The analytical error for determining $\delta^{13}C$ is ± 0,06 ‰.

Determination of dissolved and free gases

The samples collected for the measurement of free and dissolved gases were sent to the INGV-Palermo laboratory. The gases measured in these samples are CO_2, He, H_2, H_2S, O_2, N_2 and CH_4. A Perkin Elmer Clarus500 gas chromatograph equipped with a 1000 column double carboxen and TCD-FID detectors was used for these measurements. Argon (Ar) was the carrier gas used.

Determination of noble gases

Samples collected in copper pipes (according to the methodology described above) were sent to the Isotope Climatology and Environmental Research Center (ICER), Debrecen, Hungary. Measurements were made for He (^3He /^4He) and Ne (^{20}Ne / ^{22}Ne) concentrations.

The samples were coupled to the preparation line of the VG5400 Noble Gas Mass Spectrometer and the Helix device. For good measurement accuracy, the device was calibrated with air samples that have standardized concentration. The measurement error is about 1% for He and 5% for Ne (Sano & Wakita, 1985).

Data processing

The obtained data were edited with the help of the Microsoft Office package, the database related to this research was built in the Microsoft Excel program. The processing and generation of cartographic elements was performed with the QuantumGis package. To process and build images and sketches, we used the available resources generated by Windows and the PowerPoint program.

The following programs were used to interpret the generated data: Aquachem , Grapher and Surfer .

6. Results and discussions

6.1 Results obtained for water samples

The determinations of the parameters performed in-situ with WTW 350i multiparameter and the measured flows for some of the points are presented in table 1. In addition to these data, the bicarbonate concentration (HCO3) was also measured in the field, according to the methodologies described above.

Table 1. General parameters measured in the field

Cod	pH	HCO_3	EC	Eh	TDS	Sal.	Temp.	Q
		mg/L	µs/cm	mV	mg/L	‰	°C	L/s
MA 1	6.92	474.05	798	-47.6	441	0.3	22.95	nm
MA 2	7.07	564.25	1568	138.2	732	0.7	28.78	nm
MA 3	6.24	1004.25	1572	-0.45	994.5	0.7	16.03	0.24
MA 4	6.66	693.18	1383	30	860	0.8	14.7	nm
MA 5	6.295	975.95	1545.5	-41.8	945.5	0.8	20.6	0.66
MA 6	6.37	739.15	1345.5	11.35	759.5	0.7	23.34	1.77
MA 7	6.37	643.95	1305	-10.3	760	0.7	21.085	0.05
MA 8	6.68	517.6	897	-20.5	516	0.6	20.255	nm
MA 9	7.765	351.77	606	-26.95	378	0.3	15.915	nm
MA 10	6.58	549.2	945	-24.95	502.5	0.4	28.02	0.07
MA 11	6.58	585.8	969	16.1	520.5	0.4	28.37	1.09
MA 12	6.625	543.75	963	-3.8	519.5	0.4	27.45	0.23
MA 13	7.155	537	778	-2.85	471	0.4	16.135	nm
MA 14	6.59	633.95	1047.5	5.1	538	0.4	31.85	1.53
MA 15	6.4	601.05	966.5	1.9	515.5	0.4	27.55	1
MA 16	6.56	594.95	983	-3.3	523	0.4	28.955	2.98
MA 17	8.01	203.9	534	-68	343	0.2	10.95	nm
MA 18	8.8	115.9	1179.5	-125.9	753.5	0.5	32.7	0.4
MA 19	7.41	327.65	433	-41.6	287	0.1	32.6	0.64
MA 20	7.91	116.4	158.5	-56.65	101.5	0.0	22.85	2.46
MA 21	7.76	74.35	148.35	-51.4	95	0.0	26.3	5.72
MA 22	7.48	89.6	146.7	-49.6	93.5	0.0	24.7	0.16
MA 23	7.66	101.8	145.7	-49.4	93.5	0.0	25.2	0.38
MA 24	7.67	71.8	151.95	-46.3	98	0.0	26.05	nm
MA 25	7.76	107.9	148.6	-57.85	96	0.0	23.8	1.61
MA 26	8.07	67.5	350.5	-81.2	224	0.1	11.1	0.66
MA 27	7.11	24.5	1181	-27.8	757	0.6	44.5	nm
MA 28	6.92	229.4	353	-17.3	225.5	0.1	79.85	4.41
MA 29	7.5	260.55	362	-60.45	231	0.1	23.6	0.87
MA 30	8.67	408.7	243.5	-123.15	155.5	0.0	16.5	0.08
MA 31	8.42	324.6	271	-101.8	180	0.0	17.8	0.26
MA 32	8.345	574.05	392.5	-97.05	251	0.1	15.9	0.11
MA 33	8.44	549.65	398	-101.65	255.5	0.1	14.65	0.14
MA 34	7.45	3318.4	2040	-43.65	1310.5	1.0	18.55	0.19

MA 35	6.97	323.95	478.5	-25.45	307.5	0.2	34.45	0.38
MA 36	6.6	301.5	491	5	318	0.2	37.8	nm
MA 37	7.8	503.9	531.5	-69.3	341	0.2	39.6	4
MA 38	6.67	212.2	761	-3.5	489	0.3	20.1	0.04
MA 39	7.97	2754.15	190	-75.1	190	0.0	18.8	nm
MA 40	8.09	317.2	162	-78.7	104	0.0	11.4	0.23
MA 41	6.5	1631.8	1389	7.7	889	0.6	14.5	0.81
MA 42	6.16	1223.05	733	26.4	468	0.3	11.2	0.03

After the analysis of the parameters presented in table 1, several regional homogeneities were observed. A first parameter that highlights these regional differences is pH. There is a collective difference between the points located in the south of the Apuseni Mountains (Călan, Geoagiu, Rapolt) and the other points on the study area.

For the above-mentioned area, almost all the measured points have pH values between 6 and 7. Points MA 9 and MA 13 differ from this regional trend and have values between 7 and 8. To a large extent, the points from the study areas have a higher for pH, with values between 7 and 9.

The values obtained for the bicarbonate concentration denote the same regional difference between the southern and northern point groups. The southern points in the vicinity of the Mureș Valley have mainly values between 500 mg/L and 1000 mg/L, and the points in the other regions have lower values, with some exceptions. An eloquent example that represents such an exception is point MA 34 from Ceica locality. This point has a high bicarbonate concentration of 3318.4 mg/L. The waters in the Moneasa area have a low concentration of bicarbonates, which is around 100 mg/L.

For the redox potential (Eh) no regional homogeneities can be highlighted. This parameter varies significantly even for points in the same region.

The salinity of the tested points has small values, rarely exceeding 0.5 ‰, in the Moneasa area this parameter has a small value of maximum 0.1 ‰. The highest value was recorded at Ceica in point MA 34, where the salinity is 1 ‰.

The temperatures of the measured points differ significantly, with variations between 10 ° C and 80 ° C. These temperature differences can be attributed to several factors (the geothermal system of origin, the depth from which these waters come, the mixing with

surface cold water, the type of exploitation, etc.). Strictly based on this parameter we cannot make extrapolations or relevant classifications of points.

Flow rates were measured for most tested points. To correlate with the practical applications, an energy input brought by the tested geothermal sources was calculated. The methodological aspects and the results in detail are presented in Nicula et al., (2019). For the study area (points for which the flow rate and temperature are known), a total flow rate of 32.97 L/s was obtained at an average temperature of 34.05 °C. At the local level, significant flows of geothermal manifestations were identified at Geoagiu and Moneasa.

The chemical composition of the water samples

In the present research, the concentration of heavy metals is not a defining parameter of the study but can provide relevant information about the aquifer and the trajectory of geothermal fluids. Table 2 shows all the results obtained, following the sampling and analysis methodology described above.

Table 2. Concentration of heavy metals in water samples

Cod	Zn	Pb	Cd	Cr	Ni	Cu	Fe
	mg/L	mg/L	µg/L	mg/L	mg/L	mg/L	mg/L
MA 1	0.028	0.058	sld	0.019	0.007	sld	0.155
MA 2	0.029	0.053	0.206	0.042	0.008	sld	0.159
MA 3	0.039	0.054	sld	0.037	0.040	sld	0.170
MA 4	0.082	0.051	0.125	0.016	0.037	0.468	0.138
MA 5	0.041	0.049	0.049	0.023	0.025	sld	0.264
MA 6	0.086	0.046	0.011	0.021	0.054	sld	0.195
MA 7	0.046	0.063	0.043	0.001	0.023	sld	0.137
MA 8	0.035	0.038	0.016	0.018	0.040	sld	0.144
MA 9	0.023	0.048	0.004	sld	0.032	sld	0.167
MA 10	0.033	0.059	0.059	0.008	0.025	sld	0.181
MA 11	0.033	0.051	0.056	0.014	0.009	sld	0.158
MA 12	0.037	0.054	0.256	0.003	0.014	sld	0.197
MA 13	0.040	0.043	0.020	sld	0.020	sld	0.141
MA 14	0.041	0.040	0.037	0.019	0.028	sld	0.152
MA 15	0.036	0.039	0.019	0.015	0.015	sld	0.146
MA 16	0.034	0.045	0.038	0.004	0.015	sld	0.160
MA 17	0.036	0.014	0.008	0.009	0.013	0.050	0.139
MA 18	0.019	0.015	sld	0.011	0.018	0.011	0.018
MA 19	0.015	0.024	0.052	0.009	0.008	0.019	0.040
MA 20	0.016	0.008	0.084	sld	0.002	0.013	0.004
MA 21	0.016	0.004	0.120	sld	0.010	0.017	0.051
MA 22	0.013	sld	0.115	0.006	0.011	0.002	0.011
MA 23	0.015	sld	0.120	0.004	0.005	0.011	0.019
MA 24	0.015	0.010	0.228	sld	0.006	0.002	0.013
MA 25	Sld	0.012	0.108	sld	0.003	0.004	0.010

MA 26	0.018	0.025	0.121	0.002	0.004	0.001	0.133
MA 27	0.031	0.064	0.119	0.013	0.015	0.002	0.343
MA 28	Sld	0.009	0.035	0.004	0.003	0.001	0.041
MA 29	0.015	0.021	0.076	0.000	0.005	0.001	0.006
MA 30	0.011	0.004	0.048	0.000	0.006	0.002	0.014
MA 31	0.010	0.006	0.061	sld	0.003	0.001	sld
MA 32	0.010	0.001	0.086	sld	0.008	0.004	0.018
MA 33	0.026	sld	0.080	0.004	0.013	0.018	0.169
MA 34	0.019	sld	0.044	0.007	0.007	0.001	0.025
MA 35	0.017	sld	0.070	0.012	0.008	0.003	0.260
MA 36	0.018	0.007	0.053	0.009	0.007	0.001	0.032
MA 37	0.027	0.019	0.080	sld	0.010	0.010	0.143
MA 38	0.018	0.006	nm	nm	0.035	0.016	0.004
MA 39	0.020	sld	nm	nm	0.001	0.010	sld
MA 40	0.015	sld	nm	nm	sld	0.050	0.011
MA 41	0.005	0.022	nm	nm	0.035	0.021	sld
MA 42	0.042	sld	nm	nm	0.044	0.013	4.970

sld - below the detection limit; nm - not measured

The measurements results show low concentrations of heavy metals. An important aspect is given by the fact that metals with high toxicity, such as lead, cadmium and nickel, have low values. The highest concentration measured was for iron and indicates a value of 4,970 mg/L. This value was found in the Pădurea Neagră for point MA 42.

This high value is also supported by field observations (according to figure 2) and may be due to the high concentration of iron in the host rocks, as well as the presence of CO_2, which increases the ability of water to dissolve minerals.

Figura 1. Field observations on point MA 42 Pădurea Neagră

Table 3. Concentration of cations and anions in water samples

Cod	F^-	Cl^-	Br^-	NO_2^-	NO_3^-	PO_4^{3-}	SO_4^{2-}	Li^+	Na^+	NH_4^+	K^+	Mg^{2+}	Ca^{2+}
	mg/L	mg/L	mg/L	mg/L	mg/L	mg/L	mg/L	mg/L	mg/L	mg/L	mg/L	mg/L	mg/L
MA 1	sld	23.94	Sld	sld	Sld	sld	22.03	sld	31.54	Sld	sld	44.41	118.24
MA 2	1.78	140.37	Sld	sld	0.27	sld	76.17	sld	192.53	Sld	sld	24.99	88.41
MA 3	0.83	11.95	Sld	sld	Sld	sld	5.04	sld	46.44	Sld	sld	66.43	380.2
MA 4	sld	31.65	Sld	sld	17.54	sld	163.78	sld	49.66	Sld	55.59	36.44	204.13
MA 5	sld	15.24	Sld	sld	0.61	sld	4.85	sld	23.04	Sld	sld	54.97	342.23
MA 6	sld	7.34	Sld	sld	1.93	sld	8.24	sld	8.35	Sld	sld	47.02	290.66
MA 7	sld	4.82	Sld	sld	Sld	sld	10.67	sld	6.51	Sld	sld	48.98	304.34
MA 8	sld	6.1	Sld	sld	Sld	sld	14.67	sld	6.19	Sld	sld	35.99	196.26
MA 9	sld	5.32	Sld	sld	Sld	sld	13.39	sld	7.29	Sld	sld	35.65	114.41
MA 10	sld	3.91	Sld	sld	Sld	sld	13.64	sld	4.64	Sld	sld	36.17	184.38
MA 11	sld	4.86	Sld	sld	Sld	sld	16.61	sld	4.69	Sld	sld	34.94	192.15
MA 12	sld	4.92	Sld	sld	Sld	sld	8.84	sld	6.01	Sld	sld	35.33	176.74
MA 13	sld	7.3	Sld	sld	Sld	sld	20.06	sld	8.92	Sld	sld	38.41	180.12
MA 14	sld	8.03	Sld	sld	Sld	sld	18.27	sld	10.11	Sld	sld	37.81	200.66
MA 15	sld	8.42	Sld	sld	Sld	sld	18.13	sld	8.95	Sld	sld	41.55	198.69
MA 16	sld	8.08	Sld	sld	Sld	sld	16.91	sld	8.21	Sld	sld	37.01	194.41
MA 17	sld	22.86	Sld	0.61	0.72	sld	26.62	sld	27.86	Sld	3.81	9.76	40.99
MA 18	0.81	166.43	Sld	sld	0.36	sld	285.82	sld	259.69	Sld	1.14	2.45	48.71
MA 19	2.78	5.35	Sld	sld	Sld	sld	38.62	sld	61.63	Sld	2.42	13.72	38.14
MA 20	sld	11.28	Sld	sld	1.45	sld	2.19	sld	2.21	Sld	15.61	10.12	22.42
MA 21	0.05	1.4	Sld	sld	1.51	sld	2.85	sld	2.16	Sld	0.34	10.49	12.55
MA 22	0.02	1.31	Sld	sld	1.36	sld	3.21	sld	2.27	Sld	0.64	9.97	20.05
MA 23	0.02	1.53	Sld	sld	1.36	sld	3.29	sld	3.02	Sld	0.66	10.55	22.37
MA 24	0.04	2.62	Sld	sld	1.29	sld	4.33	sld	4.37	Sld	0.94	9.42	11.06
MA 25	0.03	3.43	Sld	sld	3.11	sld	3.03	sld	2.12	Sld	4.18	10.45	24.04
MA 26	0.07	3.13	Sld	sld	3.45	sld	7.03	sld	1.1	Sld	0.71	1.53	30.52
MA 27	0.81	2.79	Sld	sld	Sld	sld	875.17	sld	29.77	Sld	2.19	71.64	32.83
MA 28	0.29	17.11	Sld	sld	Sld	sld	42.75	sld	12.39	Sld	29.22	16.07	56.88
MA 29	0.32	1.95	Sld	sld	1.07	sld	17.93	sld	10.22	Sld	0.1	25.59	60.96
MA 30	0.18	2.61	Sld	sld	0.21	sld	2.76	sld	165.26	Sld	1.08	1.03	6.01

MA 31	0.06	1.45	Sld	sld	Sld	sld	2.13	sld	95.78	Sld	0.02	0.35	4.02
MA 32	0.15	1.93	Sld	sld	Sld	sld	1.06	sld	137.43	Sld	0.02	0.22	6.02
MA 33	0.31	1.97	Sld	sld	0.25	sld	0.68	sld	131.84	Sld	0.04	0.23	4.44
MA 34	0.71	23.57	Sld	sld	0.04	sld	0.37	1.06	794.23	Sld	28.31	0.42	22.12
MA 35	0.31	6.13	Sld	sld	0.43	sld	51.72	0.01	13.52	Sld	0.92	17.16	100.93
MA 36	0.49	6.5	Sld	sld	Sld	sld	75.17	sld	14.91	Sld	2.41	27.79	72.53
MA 37	0.51	30.25	Sld	sld	0.36	sld	173.1	sld	84.57	Sld	0.12	19.01	108.32
MA 38	sld	14.77	Sld	sld	2.41	sld	12.18	sld	11.68	Sld	1.58	25.17	23.66
MA 39	nm	nm	Nm	nm	Nm	nm	nm	nm	nm	Nm	nm	nm	nm
MA 40	nm	nm	Nm	nm	Nm	nm	nm	nm	nm	Nm	nm	nm	nm
MA 41	sld	260.38	Sld	sld	3.93	sld	71.65	sld	571.94	Sld	44.09	545.33	649
MA 42	nm	nm	Nm	nm	Nm	nm	nm	nm	nm	Nm	nm	nm	nm

sld - below the detection limit; nm - not measured.

Table 3 shows the results of measurements made to determine cations and anions in water samples collected during field campaigns. The data obtained were processed to obtain specific graphs and diagrams (Stiff, Piper and Giggenbach) to facilitate the interpretation of the data.

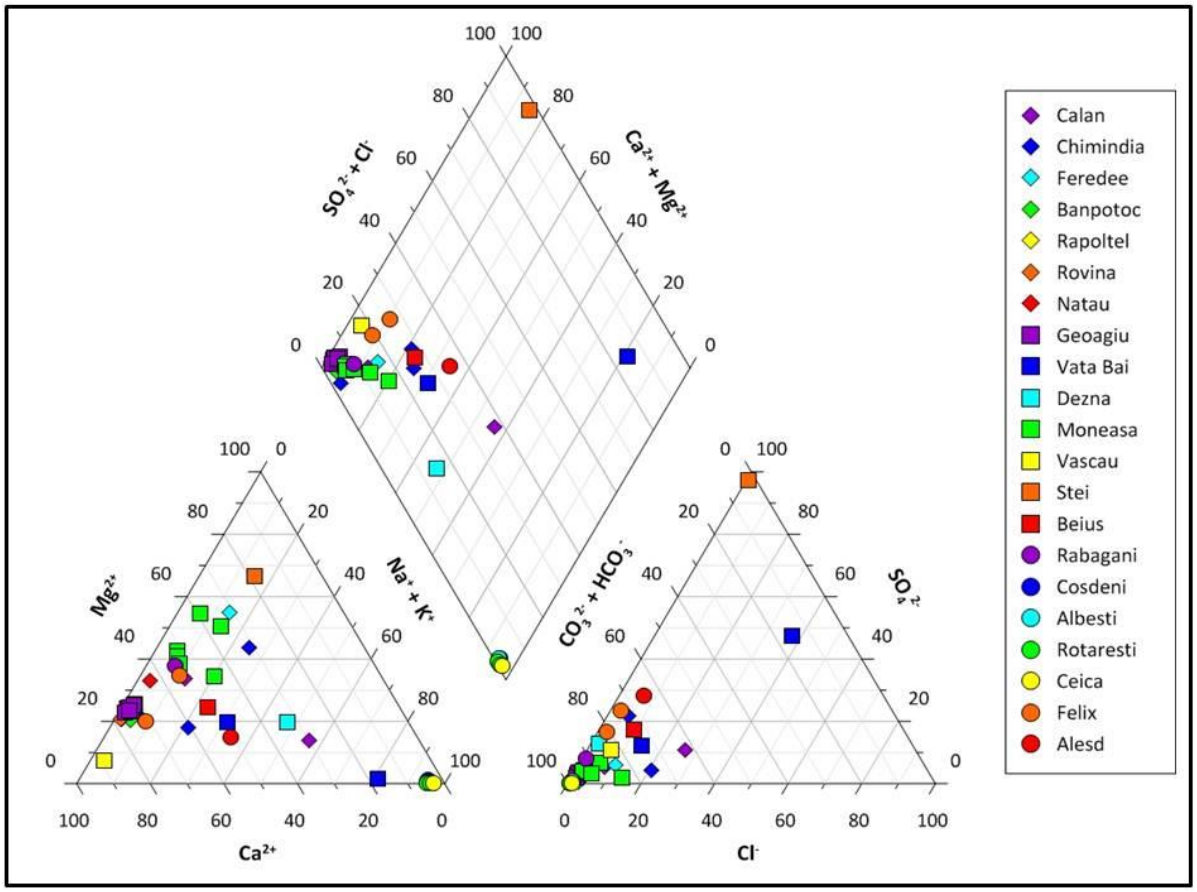

Figure 2. Piper diagram

To know the types of water and their characteristics from a geochemical point of view, the Piper diagram from figure 3 was made. This diagram shows the significant presence of bicarbonate (HCO_3) in many of the tested points. There are also points that are an exception to this trend, these points are located at Ștei MA 27 and Vața Băi MA 18. In addition to this general trend, there are two other groups, a group of points that has a higher concentration of calcium and magnesium (Ca^{2+}, Mg^{2+}) and the second group is represented by waters rich in sodium ions (Na^{+}).

Points that differ from these predominant trends have also been identified. There are points where magnesium ions predominate, and the water has a magnesium-calcium bicarbonate character (Mg^{2+}-Ca^{2+}-HCO_3). Two other types of water present on the studied area are sulphate-magnesium waters (Mg^{2+}-SO_4^{2}) and chloride-sulphates-sodium waters (Na^{+}-SO_4^{2-}-Cl^{-}).

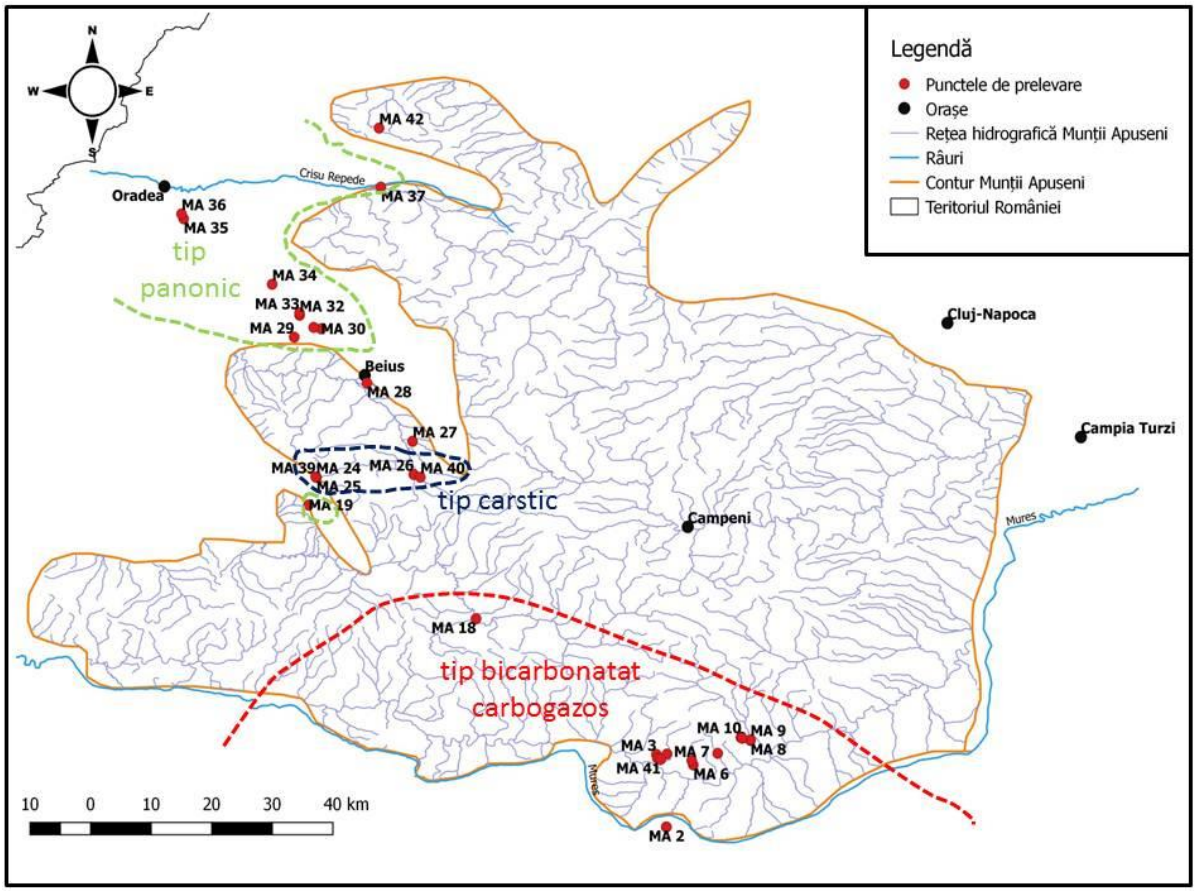

Figure 3. Hydrochemical types

In figure 4 a sketch was made with the main hydrochemical types determined in the present study. In the southern area of the Apuseni Mountains, the predominant hydrochemical type is bicarbonate-sparkling type. This type of water is representative for the samples collected from the Mureș valley area (Călan, Geoagiu, crystalline of Rapolt).

The second hydrochemical type identified in the studied area is the karstic one. This type of water is specific to the Codru-Moma Mountains area and was especially tested in Moneasa and Vașcău.

The last hydrochemical type identified is the panonic one. The waters of this type were tested in the western part of the studied area, especially they correspond to the depression areas (the three golf depressions Vad-Borod, Beiuș and Zarandului). These waters were identified at the points located in: Aleșd, Băile Felix, the northern area of the Beiuș depression and Dezna.

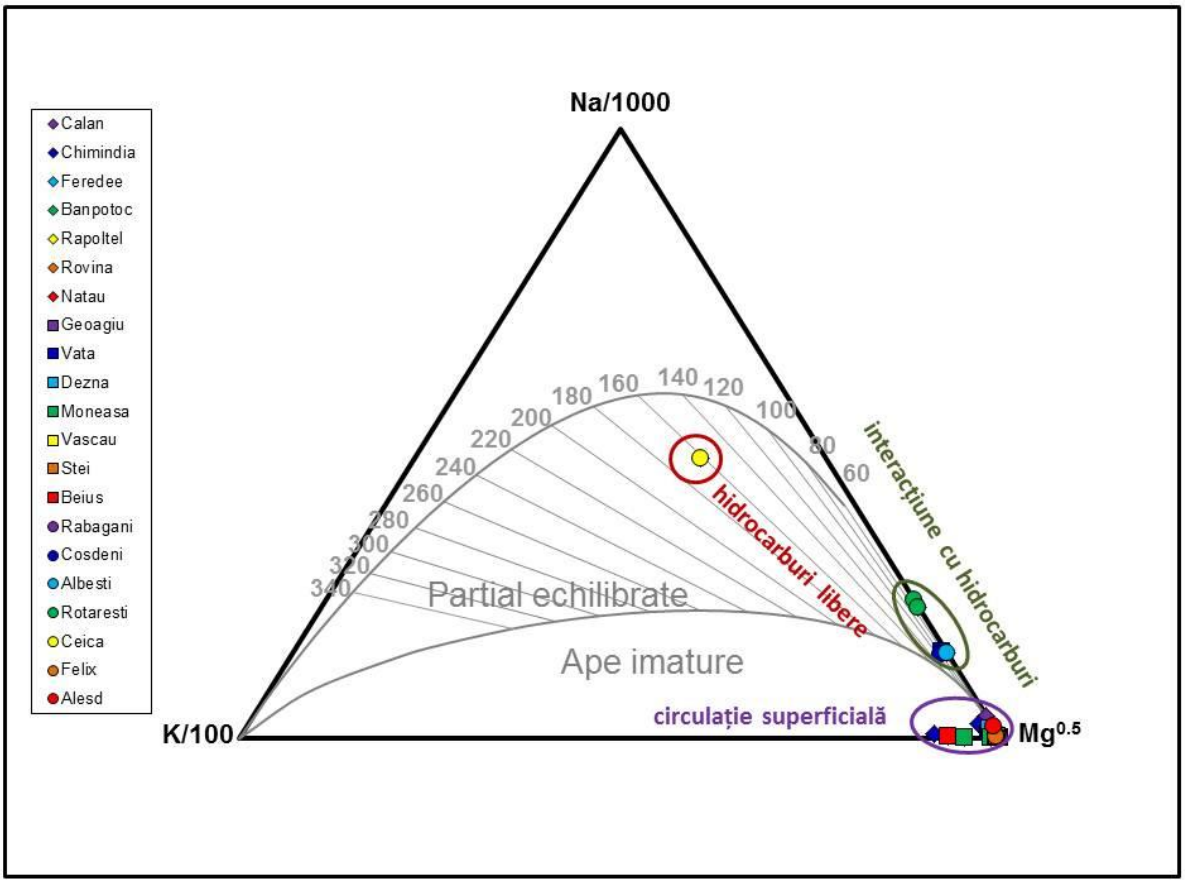

Figure 4. Giggenbach diagram (Na^{+}–K^{+}–Mg^{2+})

Except for the points in the northern part of the Beiuș Depression, the other points in the studied area contain immature waters. All these points are in the right corner of the diagram.

The points in the northern part of the Beiuș Depression (MA 30, MA 31, MA 32, MA 33, MA 34) have a different location on the Giggenbach diagram generated especially by the different concentrations of magnesium and sodium cations. The high sodium concentration of these points can be attributed to the interaction with hydrocarbon deposits.

Isotopic composition of water

According to the methodology presented above, water samples were collected and analysed to establish the isotopic composition ($\delta^{18}O$, $\delta^{2}H$). Forty-one points were included in these isotopic samples. The isotopic compositions of the analysed points are given in table 4.

Table 4. Isotopic composition of water samples

Cod	$\delta^{18}O$	SD $\delta^{18}O$	$\delta^{2}H$	SD $\delta^{2}H$	Sampling period
MA 1	-12.62	0.01	-84.58	0.06	10.2018
MA 2	-10.95	0.01	-72.38	0.10	10.2018
MA 3	-11.63	0.01	-75.58	0.16	10.2018
MA 4	-10.44	0.03	-69.48	0.11	10.2018
MA 5	-11.54	0.02	-74.72	0.04	10.2018
MA 6	-11.57	0.02	-74.82	0.08	10.2018
MA 7	-11.58	0.03	-74.67	0.09	10.2018
MA 8	-11.61	0.03	-75.35	0.12	10.2018
MA 9	nm	nm	nm	nm	nm
MA 10	-11.63	0.02	-75.10	0.07	10.2018
MA 11	-11.56	0.02	-75.05	0.29	10.2018
MA 12	-11.62	0.03	-75.40	0.04	10.2018
MA 13	-11.26	0.02	-73.31	0.13	10.2018
MA 14	-11.62	0.03	-75.11	0.17	10.2018
MA 15	-11.52	0.02	-74.81	0.05	10.2018
MA 16	-11.59	0.01	-75.18	0.07	10.2018
MA 17	-9.54	0.03	-64.63	0.08	02.2019
MA 18	-11.03	0.02	-77.35	0.05	02.2019
MA 19	-10.94	0.03	-74.96	0.05	02.2019
MA 20	-11.10	0.04	-73.15	0.15	02.2019
MA 21	-10.97	0.01	-72.49	0.03	02.2019
MA 22	-11.03	0.01	-72.72	0.05	02.2019
MA 23	-10.73	0.02	-72.17	0.07	02.2019
MA 24	-10.93	0.03	-72.64	0.21	02.2019
MA 25	-11.07	0.01	-73.03	0.15	02.2019
MA 26	-9.51	0.05	-65.50	0.09	02.2019
MA 27	-11.25	0.04	-78.96	0.05	02.2019
MA 28	-10.60	0.03	-72.13	0.09	02.2019
MA 29	-10.69	0.01	-72.27	0.16	02.2019
MA 30	-11.49	0.04	-78.39	0.14	02.2019
MA 31	-11.09	0.02	-77.92	0.05	02.2019
MA 32	-11.53	0.03	-79.60	0.09	02.2019
MA 33	-11.49	0.03	-79.56	0.09	02.2019
MA 34	-10.93	0.02	-74.95	0.16	02.2019
MA 35	-10.39	0.03	-69.49	0.06	02.2019
MA 36	-10.37	0.03	-69.62	0.08	02.2019
MA 37	-10.52	0.03	-76.42	0.09	02.2019
MA 38	-12.08	0.03	-83.49	0.12	11.2019
MA 39	-10.58	0.05	-71.75	0.09	11.2019
MA 40	-10.35	0.03	-68.93	0.03	11.2019

MA 41	-10.74	0.03	-73.31	0.08	11.2019
MA 42	-10.58	0.05	-71.75	0.09	11.2019

nm - not measured.

Figure 6 shows the isotopic composition of the main points analysed (according to the data in the table above) and is compared with the global meteoric water line (GMWL) and local meteoric water line (LMWL), Roșia Montană which is close to the studied area.

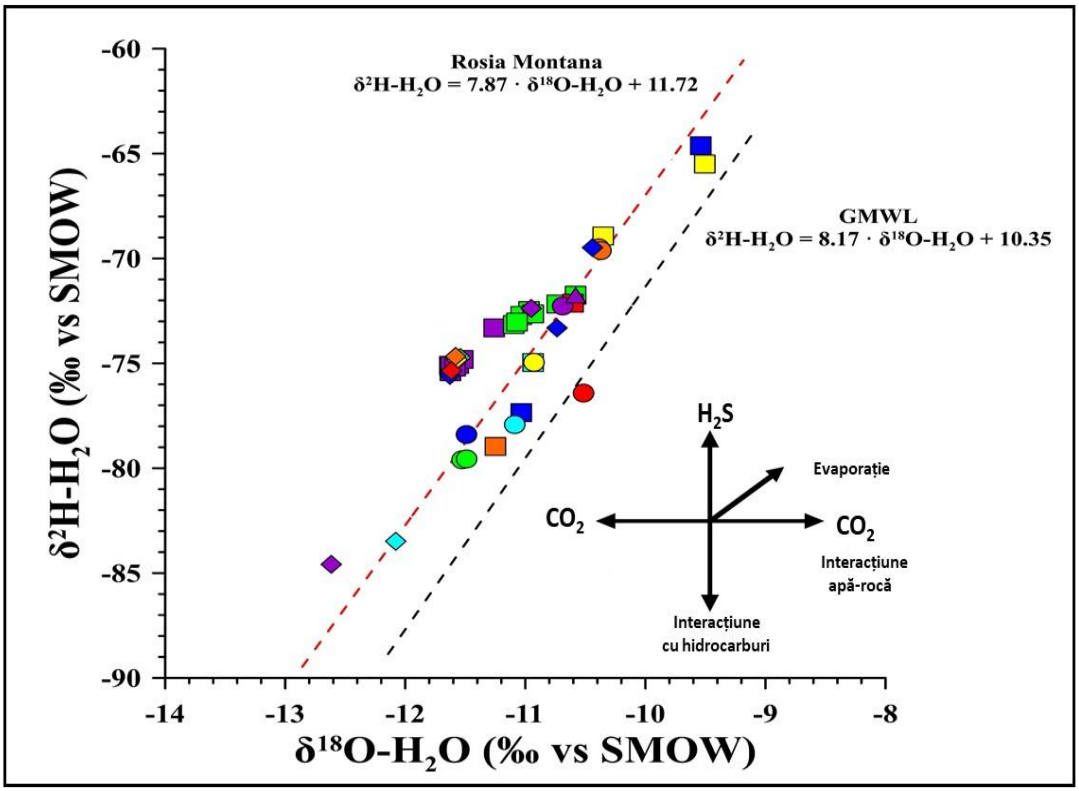

Figure 5. Isotopic composition of collected samples

Figure 6 shows the local meteoric water line (LMWL) Roșia Montană after Cozma et al., (2017). For the global meteoric water line (GMWL) was used the equation established by Rozanski et al., (1993) after the model of Craig (1961). Isotopic composition of the sampled waters has variations depending on the positioning of the point (geographical, geological).

Some of the tested points have waters that are accompanied by carbon dioxide emissions. Samples from lower temperature aquifers have carbon dioxide emissions with a lower $\delta^{18}O$ content. For this type of samples, grouping on the left side of the LMWL is specified. Water samples from higher temperature aquifers have carbon dioxide emissions with a higher $\delta^{18}O$ content. These samples are usually located on the right side of the LMWL.

According to the isotopic data obtained, points are highlighted that have similar characteristics only at the local level. Eloquent examples in this sense are the points tested at Geoagiu Băi or those tested at Moneasa.

6.2 Results obtained for gas samples

According to the methodology, samples were collected for the determination of free gases, isotopic characterization of dissolved gases and dissolved gases in water.

Gas sampling for isotopic analysis has certain more special requirements to avoid contamination and which in some cases are conditioned by the nature of the source. Because of this, no samples were collected from all points. To collect the samples necessary for the determination of the dissolved gases, it is important to avoid prolonged contact with atmospheric air or conditions which facilitate the degassing of the water and possible mixing conditions with another water. To comply with these requirements, the points that had a permanent flow (constant flow) and that had a full or almost full flow pipe section were considered relevant.

The following points were collected and analysed for dissolved gases in optimal parameters: MA 18, MA 19, MA 21, MA 28, MA 31, MA 33, MA 34, MA 35, MA 42. For free gases, sampling and analysis was conditioned by their presence and access to them. The points tested for this category are: MA 1, MA 5, MA 8, MA 21, MA 28, MA 34, MA 35, MA 38.

Table 5 shows the values resulting from the measurements of the dissolved gases in the water samples collected.

Table 5. Chemical composition of dissolved gases

Cod	H_2	O_2	N_2	CO	CH_4	CO_2
	ppm	ppm	ppm	ppm	ppm	ppm
MA 3	286	126725.99	506993.34	0.00	2.03	365993.13
MA 5	0	126964.49	567970.92	0.00	0.00	305064.58
MA 6	182	137315.14	624329.85	0.00	1.23	238172.23
MA 7	531	131124.55	640629.03	0.00	0.00	227715.30
MA 8	465	173539.91	774825.97	0.00	5.45	51163.71
MA 10	309	175946.59	733116.19	0.00	8.23	90619.86
MA 11	0	161574.26	742501.07	0.00	0.00	95924.65
MA 12	392	185463.80	789687.49	1.27	1.38	24454.40
MA 13	699	192140.27	762532.93	0.00	1.02	44627.09

MA 16	481	170097.93	737517.93	0.00	4.05	91899.55
MA 18	6.18	200035.38	799172.65	0.00	6.30	779.48
MA 19	108	190584.35	796493.08	0.00	7.42	12806.87
MA 21	1595	224090.10	772303.33	0.00	1.83	2009.76
MA 28	103	191268.52	805777.37	0.00	35.2	2816.07
MA 29	1044	204279.84	784217.18	0.00	1.70	10457.24
MA 30	47.6	153118.78	841052.65	0.00	0.00	5780.92
MA 31	325	127488.55	865583.79	0.00	12.2	6590.47
MA 32	501	151623.54	833481.17	2.03	12.4	14380.32
MA 33	207	9939.13	977464.86	0.00	8.41	12380.18
MA 34	52.4	17955.29	880085.91	0.00	46329	55577.26
MA 35	520	201992.33	779084.51	0.00	1.45	18401.41
MA 37	597	194334.44	800460.42	0.00	1.17	4606.67
MA 38	150	180699.03	741070.11	0.00	5.92	78075.34
MA 39	902	208265.98	788895.44	0.00	1.21	1935.78
MA 40	1924	267496.22	727571.23	0.00	2.13	3006.27
MA 41	743	148240.66	657540.12	1.59	1.34	193473.57
MA 42	560	53639.09	360218.66	0.00	197	585385.95

In total, the dissolved gas concentration was measured for 27 points. The dissolved gases measured for these points are: He, H_2, O_2, N_2, CO, CH_4, CO_2.

Helium was absent from all samples analysed. Carbon monoxide was also almost non-existent, it was identified in only three samples, and its concentration was low, with values between 1.27 ppm and 2.03 ppm. Oxygen, nitrogen, and carbon dioxide are the gases that have the most significant concentrations in all samples. The only point that is an exception to this rule is MA 34 (Ceica) which has a methane concentration of over 45 ppm, being the 3rd largest gas after nitrogen and carbon dioxide. The points in the Geoagiu Băi area and the Rapolt area have higher concentrations of carbon dioxide compared to the points in the other areas.

Table 6 presents the isotopic values and their ratios for the dissolved noble gases in the water samples. The following points were favourable for sampling and analysis: MA 18, MA 19, MA 21, MA 28, MA 31, MA 33, MA 34, MA 35, MA 42.

Table 6. Isotopic values and ratios for dissolved gases

Cod	He total	Ne total	R/Ra	$^{20}Ne/^{22}Ne$	$^{4}He/^{20}Ne$
	m^3 TPS	m^3 TPS			
MA 18	2.3324E-07	4.4579E-08	0.7896	42.174	5.4
MA 19	1.6816E-07	3.7310E-08	0.0353	41.989	4.6
MA 21	4.6913E-07	3.2562E-07	0.8484	46.942	1.5
MA 28	8.4613E-07	2.7499E-08	0.0905	42.185	31.6

MA 30	1.8369E-07	7.7522E-08	0.1032	42.043	2.4
MA 33	5.3168E-07	5.8071E-07	0.5596	13.281	1.0
MA 34	1.5875E-07	6.4359E-08	0.0596	42.017	2.5
MA 35	1.0138E-07	2.7591E-11	1.3607	727.003	3689.2
MA 42	2.3365E-07	5.0555E-09	1.7810	42.603	47.4

TPS - Standard temperature and pressure

Mostly the points presented in table 6 come from different areas (geological and geographical). This can also influence the concentrations of the analysed gases. It was observed that point MA 35 (Felix Parc) has different values (obvious difference compared to the ratios of the other points) for the isotopic ratios of neon and helium. Considering these aspects, we assume that in point MA 35 there is a different thermal system compared to other systems in the study area.

At some points, the presence of free gases was observed. From the points that corresponded to a correct sampling according to the methodology, free gas samples were collected and subsequently analysed. Table 7 shows the composition of these samples.

Table 7. Chemical composition of free gases

Cod	**He**	**H_2**	**O_2**	**N_2**	**CO**	**CH_4**	**CO_2**	**H_2S**	**C_2H_6**
	ppm	ppm	ppm	Ppm	ppm	ppm	ppm	ppm	ppm
MA 1	< 3	20.0	203900	768500	2.9	335.0	2900	< 1	< 10
MA 5	9	6.0	180200	671100	18.0	184	150900	< 1	< 10
MA 8	171	< 3	128800	779000	2.2	< 0.5	96200	< 1	< 10
MA 21	< 3	< 3	208400	779600	1.7	2.2	1300	< 1	< 10
MA 28	< 3	< 3	208700	783700	< 0.5	116	3400	< 1	< 10
MA 34	33	< 3	11000	744300	< 0.5	136800	85300	< 1	< 10
MA 35	< 3	< 3	145700	821100	< 0.5	14	22900	< 1	< 10
MA 38	562	< 3	26600	787400	1.6	23	179800	< 1	< 10

The measured values for free gases have the same trends as the values for dissolved gases. The predominant gases are nitrogen, oxygen, and carbon dioxide. Methane is present in high concentration only at point MA 34 (Ceica).

Table 8 presents the isotopic values for the free gases collected from Călan (MA 1) and Banpotoc (MA 5).

Table 8. Isotopic values and ratios for free gases

Cod	^{4}He	^{3}He	^{20}Ne	^{22}Ne	$^{20}Ne/^{22}Ne$	R/Ra

	ppm	ppm	ppm	ppm		
MA 1	664.7269	8.2717E-04	16.2641	1.6714	9.7307	0.8991
MA 5	10.9859	3.3092E-05	17.6356	1.8126	9.7293	2.1765

Given that there are only data on these two points, no relevant extrapolations or comparisons can be made. Point MA 5 has a higher flux of helium, which suggests a contribution of helium from the mantle.

With the data obtained for the types of gases presented above, graphs and diagrams were constructed to facilitate their interpretation and understanding, to formulate relevant conclusions.

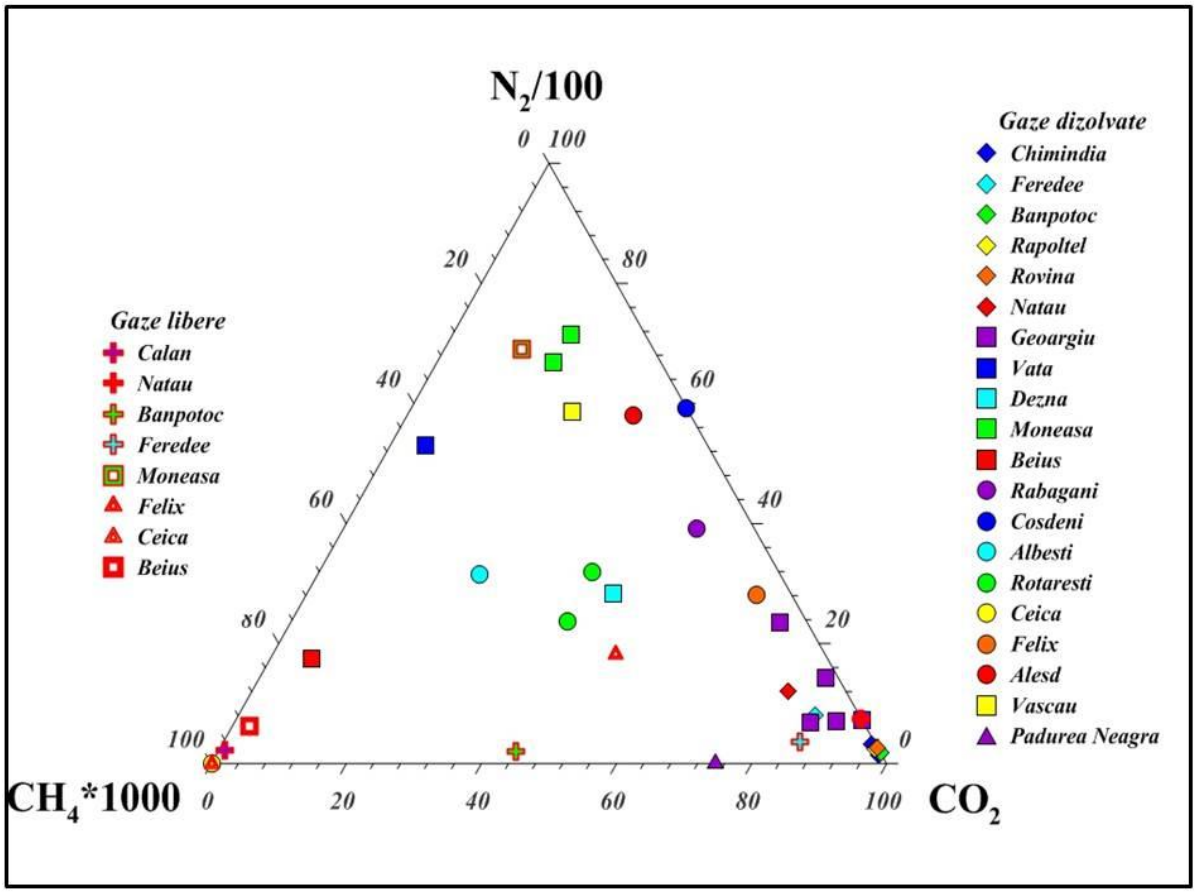

Figure 6. Ternary diagram for nitrogen-methane and carbon dioxide

Figure 7 shows with the help of a ternary diagram the concentrations of free and dissolved gases (CH4, CO2 and N2) in the collected samples. In this context, there is a directly proportional relationship between the concentration of dissolved and free gases. Some points where these proportions are eloquent are at Moneasa, Feredee, Ceica.

In terms of concentration, it is noted that a large part of the analysed points has a high concentration of carbon dioxide. Carbon dioxide is present especially at the sampling points from the south of the Apuseni Mountains. Significant concentrations of methane are found in Ceica (MA 34), Beiuș (MA 28) and Călan (MA 1).

A group of points that is highlighted by a high concentration of nitrogen is represented by the points tested at Moneasa and Vașcău. This concentration can be correlated with a shallow water circulation but also with the contact of the atmosphere. Karst gaps can facilitate this contact with atmospheric air.

In the central part of the ternary diagram there is a group of points that has a mix of the three gases represented. These points come from Albești (MA 31), Rotărești (MA 32, MA 33), Dezna (MA 19) and Felix (MA 35).

The diagram in figure 8 was constructed according to the Sano & Marty (1994) model and the $CO_2/^3He$ versus $\delta^{13}C\text{-}CO_2$ ratios were used.

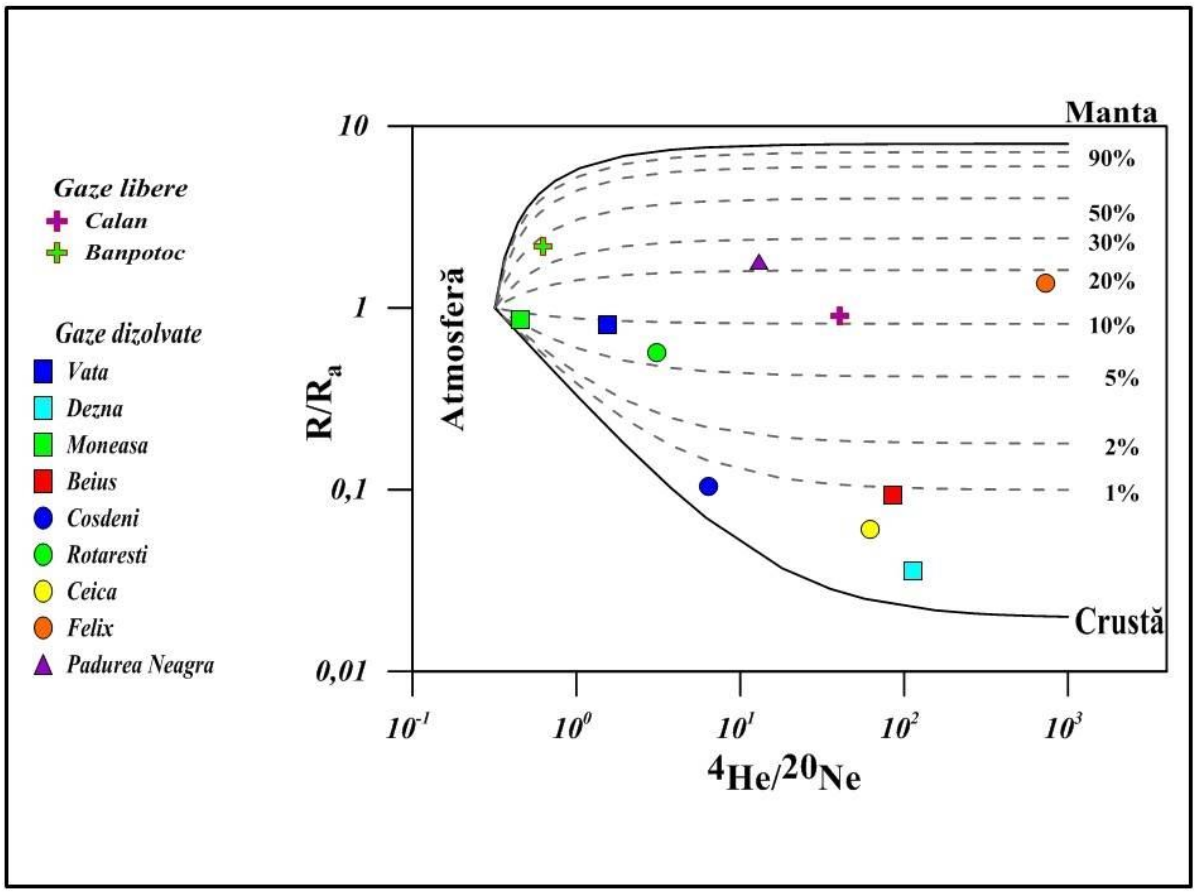

Figure 7. Diagram with ratio R/R_a on $^4He/^{20}Ne$

The diagram in figure 8 highlights the origin of the measured gases. The points that have gases of crustal origin are placed on the graph below the line of 1%. Three of the four points are in the Beiuș Depression. This provenance is identified in many cases with sedimentary deposits.

The second category consists of points located around the 10% line. These points contain a mixture of gases of crustal and mantle origin. Most of the points have a more significant atmospheric contribution (Moneasa, Vața Rotărești).

Around the line of 20% and above are the points that have a significant contribution of gases from the mantle. The identification of this type of gas indicates a communication with the mantle through different systems (faults, fractures).

7. General conclusions

Following the research presented above, we can conclude that geothermal manifestations (water and gas) are present in the studied area. The general location of these thermal areas follows an alignment approximately in the SE-NW direction, but there are also points with thermal manifestations outside this alignment.

From a quantitative point of view, these geothermal resources are sustainable for various anthropogenic uses. Their use in resilient systems can generate environmental benefits as well as economic benefits. The use of these resources varies, and studies must be carried out to demonstrate the feasibility of using them in each context.

From a geochemical point of view, the analysed samples denote a chemical variety on the studied area. The most common type of water was calcium-magnesium bicarbonate, which is found throughout the study area. Another type of water representative especially for the northern part of the Beiuș Depression is the sodium bicarbonate type. The origin of the gases present in the analysed thermal systems is mainly crustal.

Following the information and data obtained in this study, it appears that geothermal waters in the Apuseni Mountains and surrounding areas may have different genetic characteristics.

8. Bibliography

Anticsa M., Rosca M., 2003, Geothermal development in Romania, Geothermics 32 (2003), 361–370.

Arason S., 2003, The drying of fish and utilization of geothermal energy; the Icelandic experience, International Geothermal Conference, Reykjavík, (2003) 21-31.

Berdondini F., Bronzi P., Burgassi P., Marconcini R., Pignatari M., Rosenthal H., 1995, Utilization of geothermal source in a closed cycle aquaculture system in Italy: Preliminary results, World Geothermal Congress, (1995) 2309 – 2312.

Boyd T., Lund J.,2000, Geothermal Heating of Greenhouses and Aquaculture Facilities, Geothermal Resources Council Transactions, Vol. 24, September (2000) 24-27.

Butac A., Opran C., 1985, Geothermal resources in Romania and their utilizations, Geothermics, Vol.12, No.2/3, (1983) 371-377.

Colesca S., Ciocoiu C.,2013, An overview of the Romanian renewable energy sector, Renewable and Sustainable Energy Reviews 24 (2013) 149–158.

Cozma A., Baciu C., Papp D., Roșian G., Pop C.,2017, Isotopic composition of precipitation in western Transylvania (Romania) reflected by two local meteoric water lines, Carpathian Journal of Earth and Environmental Sciences, July 2017, Vol. 12, No. 2, (2017) 357-364.

Craig H., 1961, Isotope variations in meteoric waters, Science 133, 1702-1703.

Demetrescu C., Andreescu M., 1994, On the thermal regime of some tectonic units in a continental collision environment in Romania, Tectonophysics 230, (1994) 265-276.

Dumitru O., Forray F., Fornósc J., Ersek V., Onac B., 2016, Water isotopic variability in Mallorca: a path to understanding past changes in hydroclimate, Hydrological Processes Vol. 31, (2016) 104 -116.

Gheorghe Al., Crăciun P., 1993, Thermal aquifers in Romania, Journal of Hydrology, 145, (1993) 111 -123.

Ianovici V., Borcoș V., Bleahu M., Patrulius D., Lupu M., Dimitrescu R., Savu H., 1976, Geologia Muntilor Apuseni, Editura Academiei Republici Socialiste România, București.

Italiano F., Yuce G., Uysal I.T., Gasparon M., Morelli G., 2014, Insights into mantle-type volatiles contribution from dissolved gases in artesian waters of the Great Artesian Basin, Australia. Chem. Geol. 378 – 379, (2014), 75 – 88.

Lund J.E., Boyd T.L., 2016, Direct utilization of geothermal energy 2015 worldwide review, Geothermics 60, (2016) 66-93.

Mutihac V., 1990, Structura geologică a teritoriului României, Editura Tehnică, București.

Nicula A. M., Ionescu A., Pop I. C., Orășeanu I., Baciu C., 2019, Preliminary considerations regarding the geothermal potential in the Apuseni Mountains Area, Studia UBB Ambientum, LXIV, 2, (2019), 45-56.

Orășeanu I., 2016, Hidrogeologia Carstului din Munții Apuseni, Editura Belvedere, Oradea.

Papić P., 2016, Mineral and Thermal Waters of Southeastern Europe, Environmental Earth Sciences, Springer International Publishing.

Plugaru S.C.R, Dan V., Gabor T., Mentiu X.P., 2018, The use of geothermal water in the cultivation of some algae species: a review, Ecoterra 15(2),(2015) 27-33.

Rădulescu M., & Teodoreanu E., 2014, Noțiuni de balneofizioterapie și balneoclimatologie, Editura Medicală, București.

Rozanski K., Araguás-Araguás L., Gonfiantini R., 1993. Isotopic pattern in modern global precipitation, Climate Change in Continental Isotopic Records, Washington (1993), 1-37.

Sandulescu, M., 1984, Geotectonica Românieie, Editura Tehnică, Bucuresti.

Sano Y. & Wakita H.,1985, Geographical distribution of 3He/4He ratios in Japan: Implications for arc tectonics and incipient magmatism. Journal of Geophysical Research 90, doi: 10.1029.

Sano Y., Marty B., 1994, Origin of carbon in fumarolic gas from island arcs, Chemical Geology (Isotope Geoscience Section) 119, (1995) 265-274.

Schmid M., Fügenschuh B., Kounov A., Matenco L., Nievergelt P., Oberhansli R., Pleuger J., Schefer S., Schuster R., Tomljenovi B., Ustaszewski K., J.J. van Hinsbergen D., 2020, Tectonic units of the Alpine collision zone between Eastern Alps and western Turkey, Gondwana Research 78, (2020) 308-374.

Schmidl A., 1863, Das Bihar-Gebirgen an der Grenze von Ungarn und Siebenburgen, Verlag von Forster & Bartelmus, Vien.

Seghedi I., Downes H., Harangi S., Mason P., Pecskay Z., 2005, Geochemical response of magmas to Neogene–Quaternary continental collision in the Carpathian–Pannonian region: A review, Tectonophysics 410, (2005) 485 - 499.

Sordelli C., Karkoulias V., 1995, Geothermal installation in Rodigo, World Geothermal Congress, (1995) 2313-2315.

Sturza M., 1950, Manual de Balneologie, Editura de Stat.

Tiliță M., Lenkeyc L., Mațencoa L., Horváth F., Surányid G., Cloetingha S., 2018, Heat flow modelling in the Transylvanian basin: Implications for the evolution of the intra-Carpathians area, Global and Planetary Change 171, (2018) 148-166.

https://www.geothermal-energy.org/explore/our-databases/geothermal-power-database/direct-uses-by-country [accesat 16.01.2020] (IGA) International Geothermal Association

http://www.picarro.com [accessed 25.03.2020]